Global-to-Cartesian 3-D EM modeling using a nested IE approach with application to long-period responses from island geomagnetic observatories

Chaojian Chen[1], Mikhail Kruglyakov[1,2], and Alexey Kuvshinov[1]

[1] Institute of Geophysics, ETH Zurich, Switzerland (chaojian.chen@erdw.ethz.ch)

[2] Geoelectromagnetic Research Centre, Institute of Physics of the Earth, Moscow, Russia

Probing mantle conductivity using observatory data

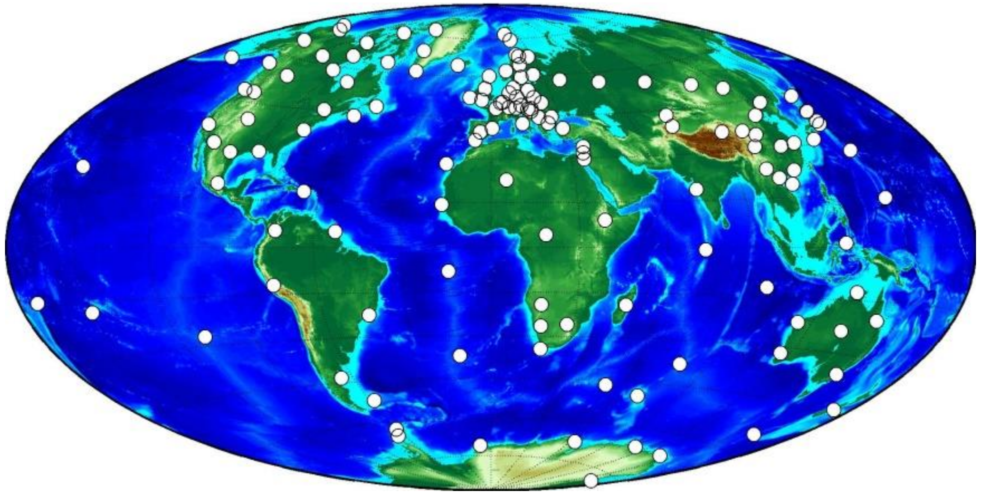

Geomagnetic observatories

- Constraining global 3-D model of uniform lateral resolution is probably not feasible due to:
  - Irregular distribution of geomagnetic observatories
  - Diffusion character of EM induction (sensitive only around locations)
- But there is a lot of interest to constrain mantle conductivity distributions beneath oceans
- What is feasible:
  - Constraining local 1-D models beneath island observatories

Deep mantle structures are obtained by inverting local C-responses

- Data to estimate C-responses is magnetic field variations in the period range between a few days and a few months due to a magnetospheric (ring current) source

- Source is described via first zonal harmonic

- Assuming this source geometry one determines the *C*-response as (Banks, 1969):

$$C(\mathbf{r}_a, w) = -\frac{a}{2}\tan\theta \frac{B_r(\mathbf{r}_a, w)}{B_\theta(\mathbf{r}_a, w)}$$

$\mathbf{r}_a = (a, \theta, \phi)$ – observatory's coordinate, w – frequency, a – the Earth's radius, θ – geomagnetic colatitude, B_r and B_θ – the radial and horizontal components of the magnetic field

Banks, R. Geophysical Journal International, 1969, 17(5): 457–487.

Challenge

- C-responses at island observatories may be strongly distorted by the ocean induction effect (OIE) originating from conductivity contrasts between ocean and land
- The OIE in C-responses is generally modeled by global thin shell simulations using relatively coarse (1^ox1^o) grid

Thin shell is used to account for the OIE

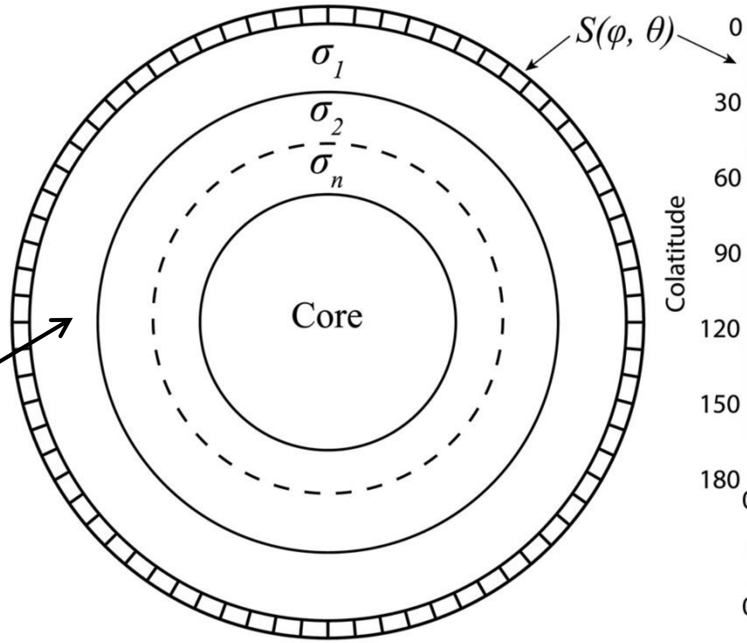

uniform 1-D layers

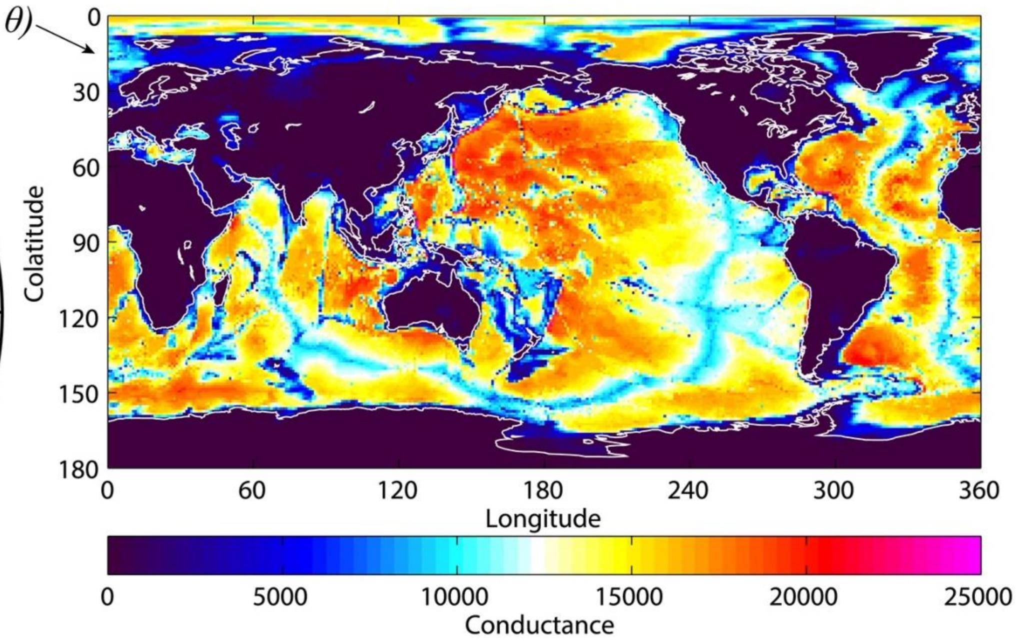

Challenge

- Noticeable disagreement between imaginary parts of modeled and observed responses at island observatories (at periods shorter than two weeks) was detected (Munch et al., 2018)

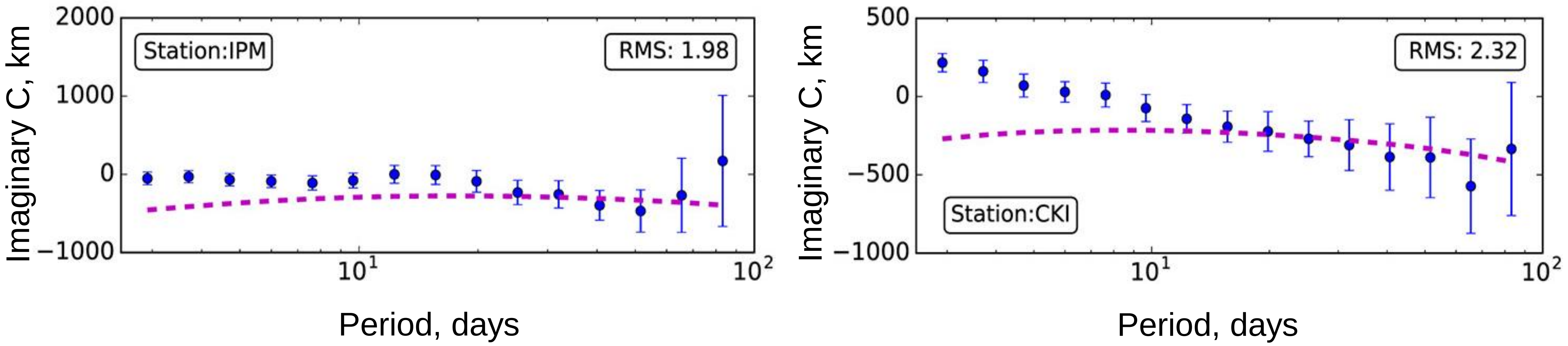

Whether the discrepancy is due to very local bathymetry that is not accounted for in "coarse (1^ox1^o) grid" modeling?

Munch, F. D., Grayver, A. V., Kuvshinov, A., & Khan, A. JGR: Solid Earth, 2018, 123(1), 31-51.

Accounting for OIE requires numerical solution of Maxwell's equations

- Maxwell's equations:

$$\nabla \times \mathbf{H}(\mathbf{r}) = \sigma(\mathbf{r})\mathbf{E}(\mathbf{r}) + \mathbf{j}^{ext}(\mathbf{r})$$

$$\nabla \times \mathbf{E}(\mathbf{r}) = i\omega\mu_0\mathbf{H}(\mathbf{r})$$

- σ : conductivity distribution
- $\mathbf{j}^{ext}$: extraneous source
- ω : angular frequency
- μ_0 : magnetic permeability of free space

- For this problem setup, integral equation method is preferred, as only discretization of thin shell is needed

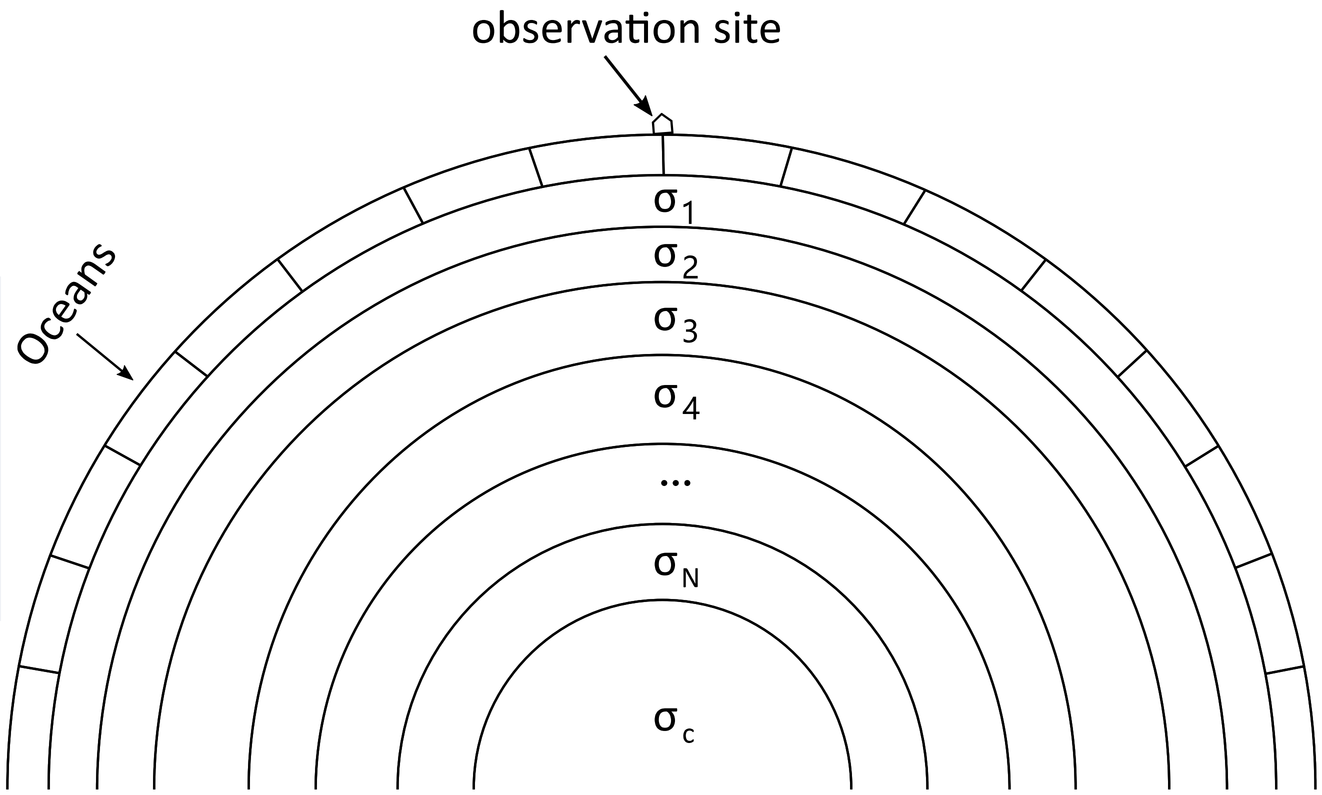

Spherical coordinates

IE method in a nutshell

- Solve numerically:

$$\mathbf{E}(\mathbf{r})-\int_{V^1}\hat{G}^{ej}(\mathbf{r},\mathbf{r}')\Delta\sigma(\mathbf{r}')\mathbf{E}(\mathbf{r}')dv'=\mathbf{E}_0(\mathbf{r}),\mathbf{r}\in V^1,\mathbf{r}'\in V^1$$

- Then, electric and magnetic fields are calculated as:

$$\mathbf{E}(\mathbf{r})=\mathbf{E}_0(\mathbf{r})+\int_{V^1}\hat{G}^{ej}(\mathbf{r},\mathbf{r}')\Delta\sigma(\mathbf{r}')\mathbf{E}(\mathbf{r}')dv'$$

$$\mathbf{H}(\mathbf{r})=\mathbf{H}_0(\mathbf{r})+\int_{V^1}\hat{G}^{hj}(\mathbf{r},\mathbf{r}')\Delta\sigma(\mathbf{r}')\mathbf{E}(\mathbf{r}')dv'$$

$\mathbf{E}_0,\mathbf{H}_0$: background electric and magnetic fields

$\hat{G}^{ej},\hat{G}^{hj}$: electric and magnetic Green's tensors

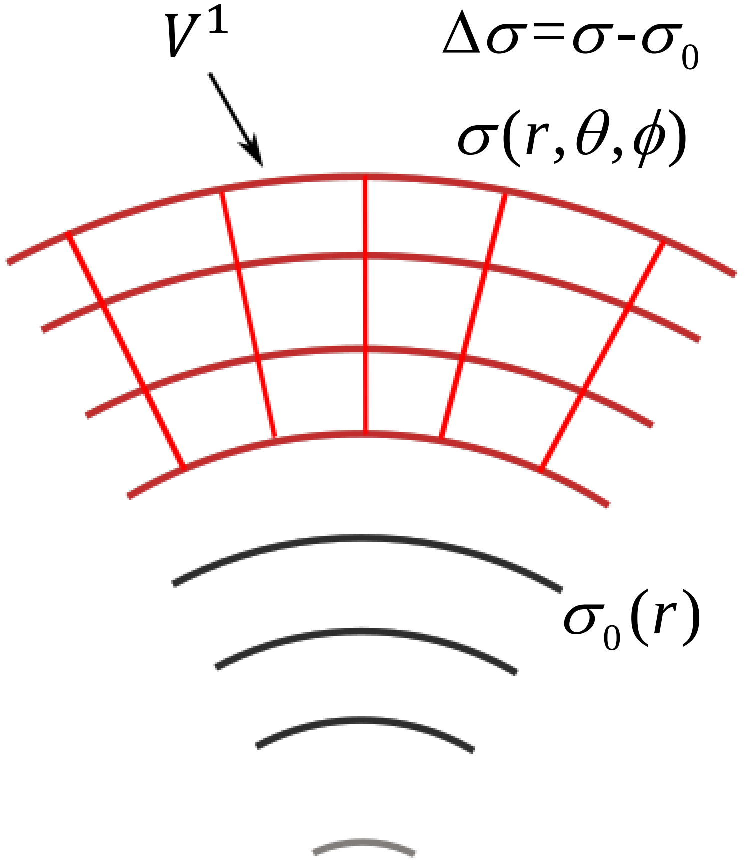

Using fast Fourier transform (FFT) dramatically decreases computational loads (both in time and memory)

Challenge with existing FFT-based IE

- Three ways to account for the very local 3-D effects within IE approach

1) FFT, uniformly fine grid (computationally expensive)

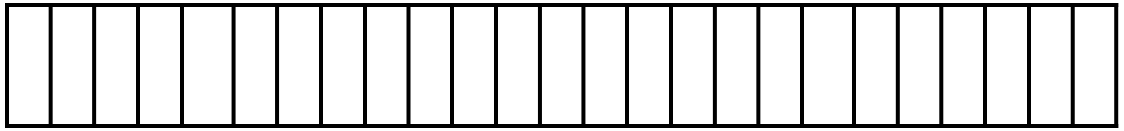

2) No FFT, adaptive grid (computationally expensive)

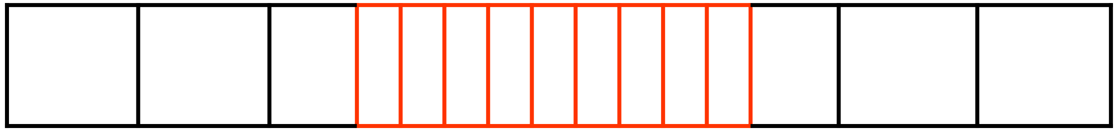

- Step 1: FFT, uniformly coarse grid

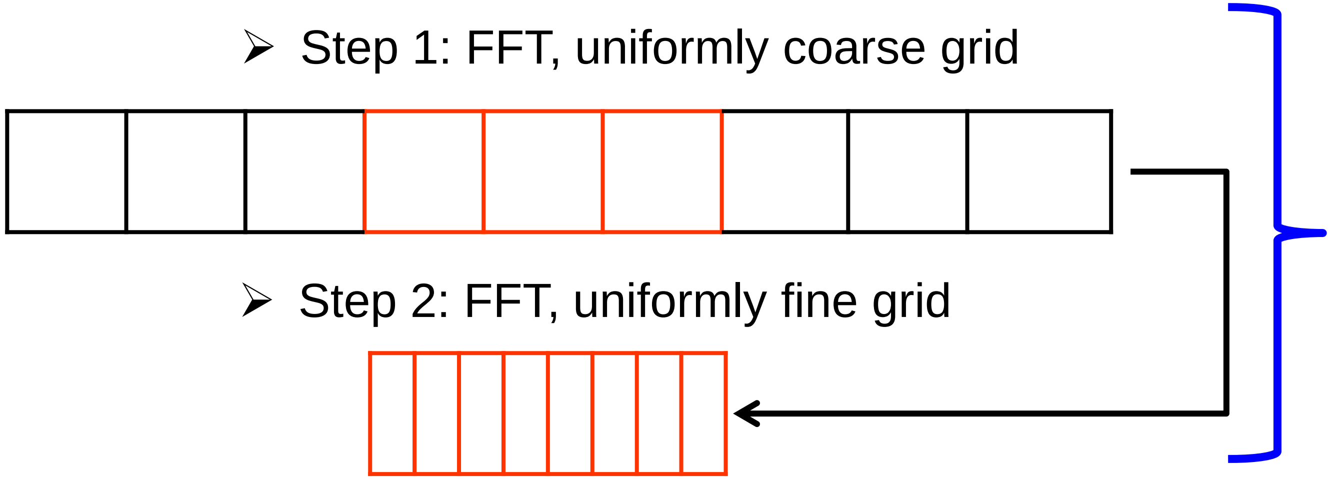

- Step 2: FFT, uniformly fine grid

3) Nested IE approach (computationally efficient)

Nested IE approach

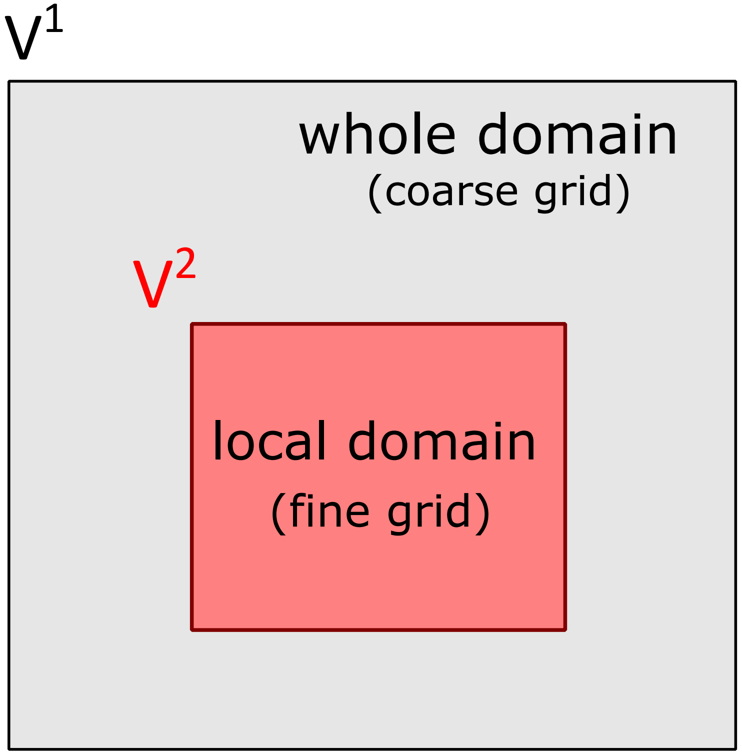

- Calculate EM field in the whole domain $(\mathbf{r} \in V^1)$ on a coarse grid

$$\mathbf{E}^{(c)}(\mathbf{r}) - \int_{V^1} \hat{G}^{ej(c)}(\mathbf{r},\mathbf{r}')\Delta\sigma^{(c)}(\mathbf{r}')\mathbf{E}^{(c)}(\mathbf{r}')dv' = \mathbf{E}_0^{(c)}(\mathbf{r})$$

- Calculate EM field in the local domain $(\mathbf{r} \in V^2)$ on a fine grid

$$\mathbf{E}^{(f)}(\mathbf{r}) - \int_{V_2} \hat{G}^{ej(f)}(\mathbf{r},\mathbf{r}')\Delta\sigma^{(f)}(\mathbf{r}')\mathbf{E}^{(f)}(\mathbf{r}')dv' = \boxed{P_c^f\left[\mathbf{E}_0^{(c)}(\mathbf{r}) + \mathbf{E}^{add(c)}(\mathbf{r})\right]}$$

$$\mathbf{E}^{add(c)}(\mathbf{r}) = \int_{V_1/V_2} \hat{G}^{ej(c)}(\mathbf{r},\mathbf{r}')\Delta\sigma^{(c)}(\mathbf{r}')\mathbf{E}^{(c)}(\mathbf{r}')dv'$$

P_c^f: projection operator

Global-to-Cartesian (G2C) approach

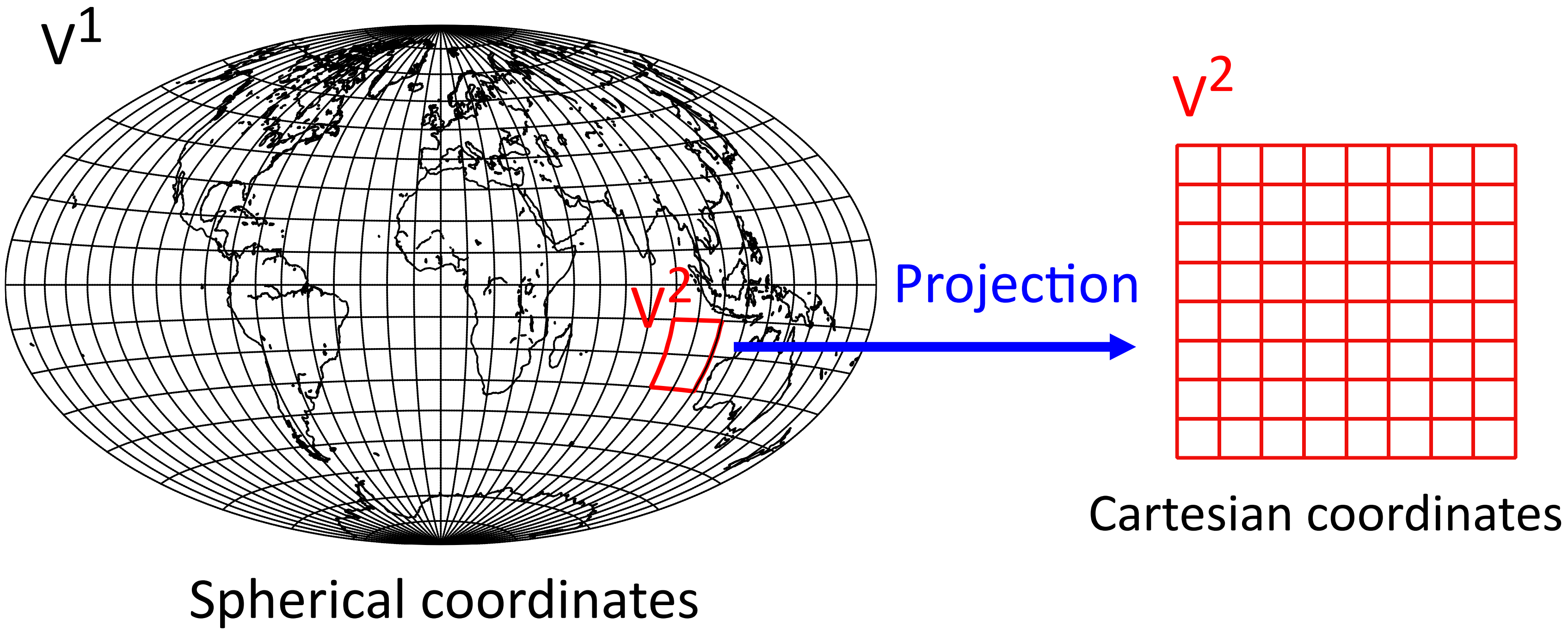

① Global (spherical) IE solver: X3DG (Kuvshinov, 2008)

② Regional (Cartesian) IE solver: PGIEM2G (Kruglyakov & Kuvshinov, 2018)

Kuvshinov, A. V. Surveys in Geophysics, 2008, 29(2), 139-186.
Kruglyakov, M., & Kuvshinov, A. Geophysical Journal International, 2018, 213(2), 1387-1401.

Modeling C-responses at CKI and HON

- Spherical grid: 1º x 1º
- Cartesian grids: from 1º x 1º (100 km x 100 km) to 0.01º x 0.01º (1 km x 1 km)
- 1-D profiles beneath CKI and HON are taken from Munch et al., (2018)

Global 1º x 1º **conductance distribution**

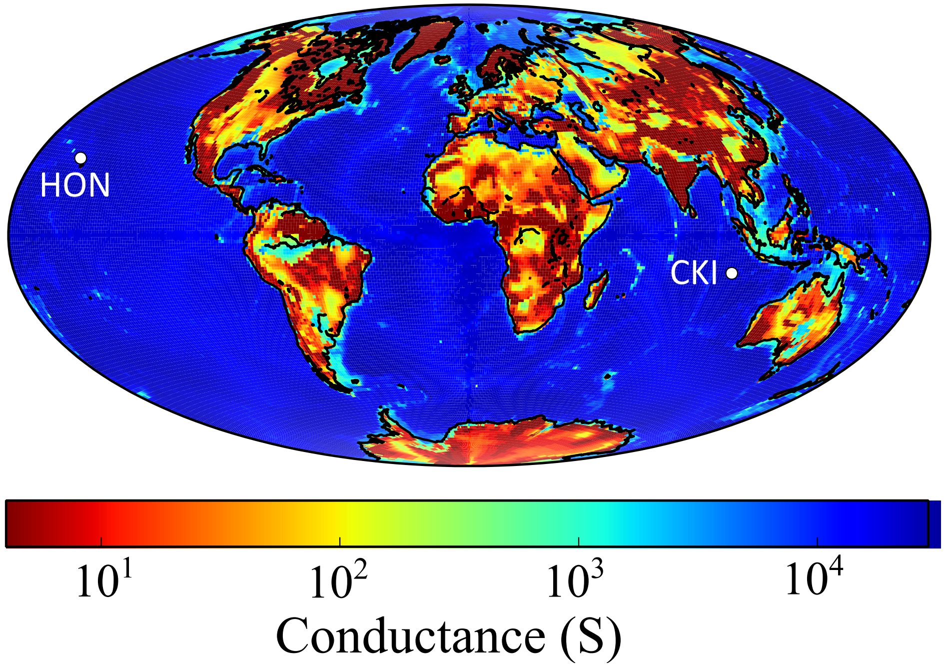

Local 1 km x 1 km conductance distribution

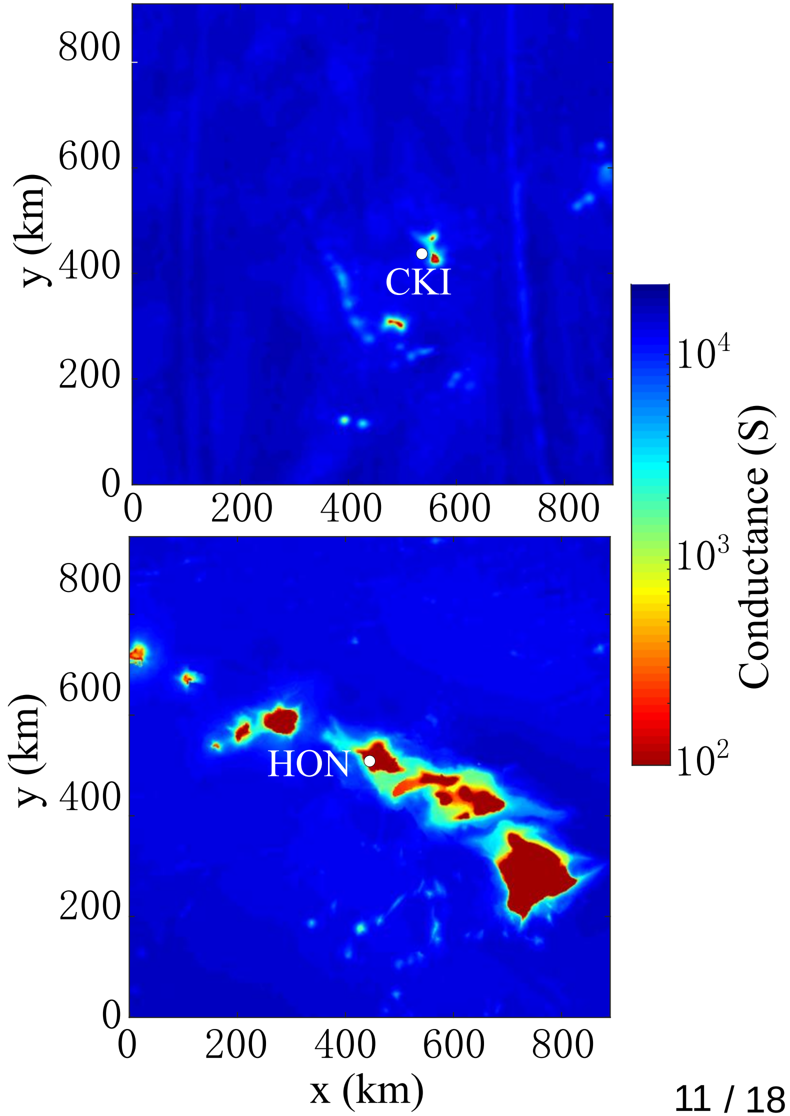

OIE in C-responses at CKI

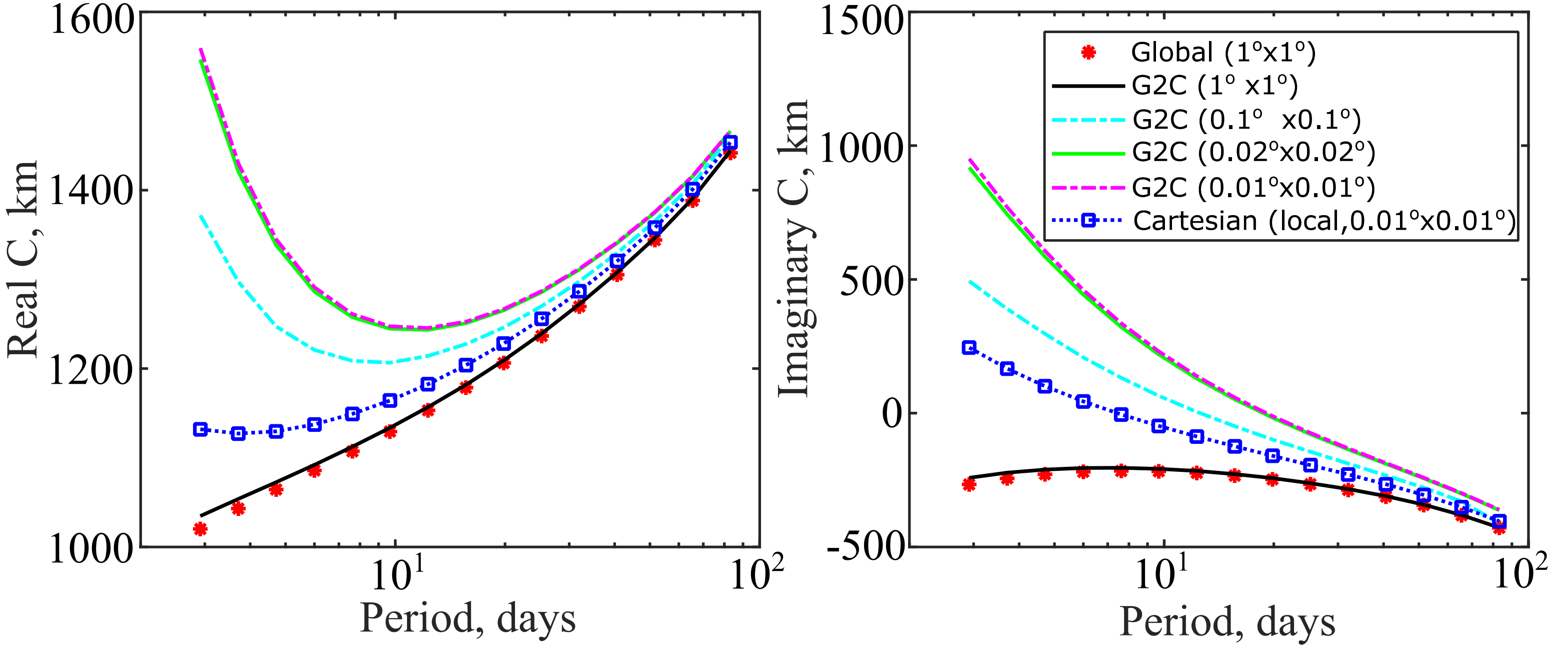

- Good agreement of responses calculated by global and G2C approaches using the same grid of 1º x 1º validates the G2C approach
- C-responses modeled at different grids differ much but “saturation” occurs at grid of 0.02º x 0.02º
- C-responses modeled using only local (Cartesian) domain differ from those modeled with G2C tool

OIE in C-responses at HON

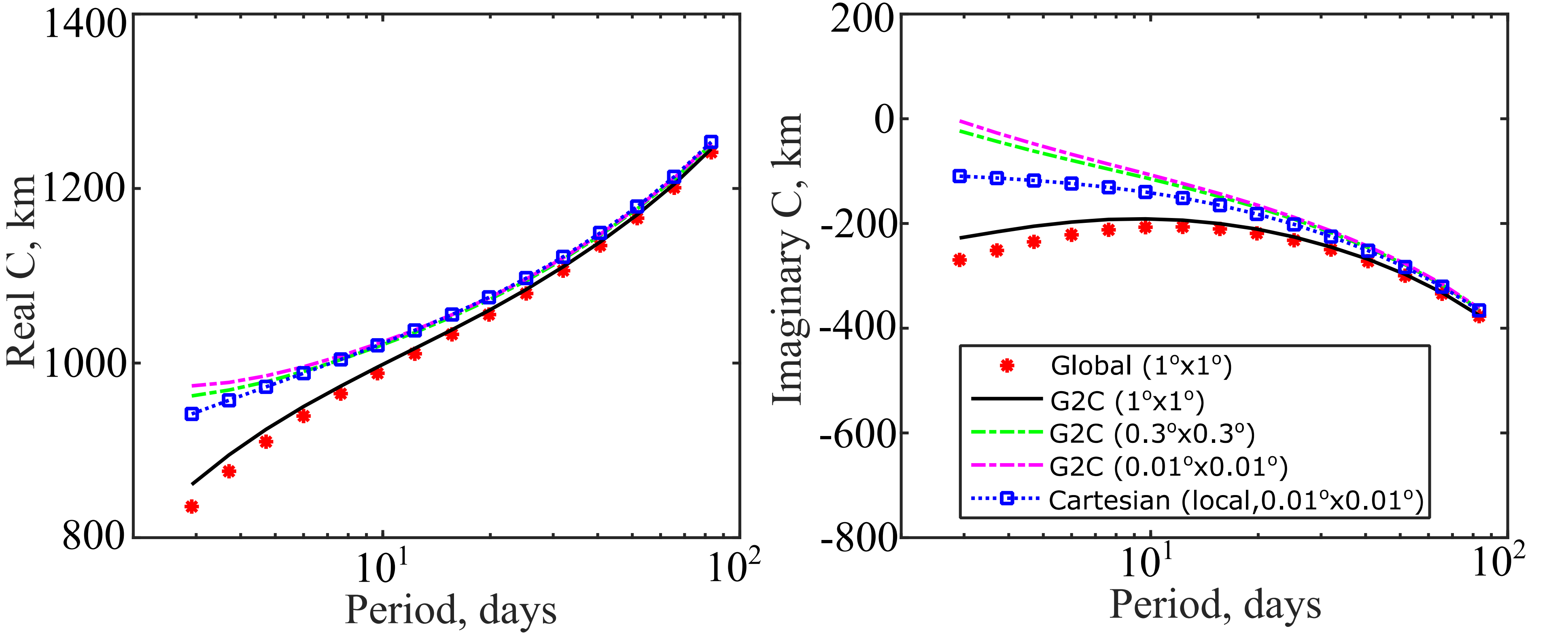

➢ For HON observatory, conductance resolution of 0.3° x 0.3° is sufficient to account for the OIE

Obtaining new 1-D profiles beneath CKI and HON

- Correction of observed C-responses

$$C^{\text{obs,corr}}(\mathbf{r}_a, w) = C^{\text{obs}}(\mathbf{r}_a, w) \cdot \frac{C^{\text{1D}}(\mathbf{r}_a, w)}{C^{\text{1D+shell}}(\mathbf{r}_a, w)}$$

C^{1D} : C-responses computed using 1-D profile obtained by Munch et al., (2018)

$C^{\text{1D+shell}}$: C-responses computed using 1-D profile overlaid by laterally non-uniform surface shell

- 1-D inversion of the corrected responses $C^{\text{obs,corr}}$

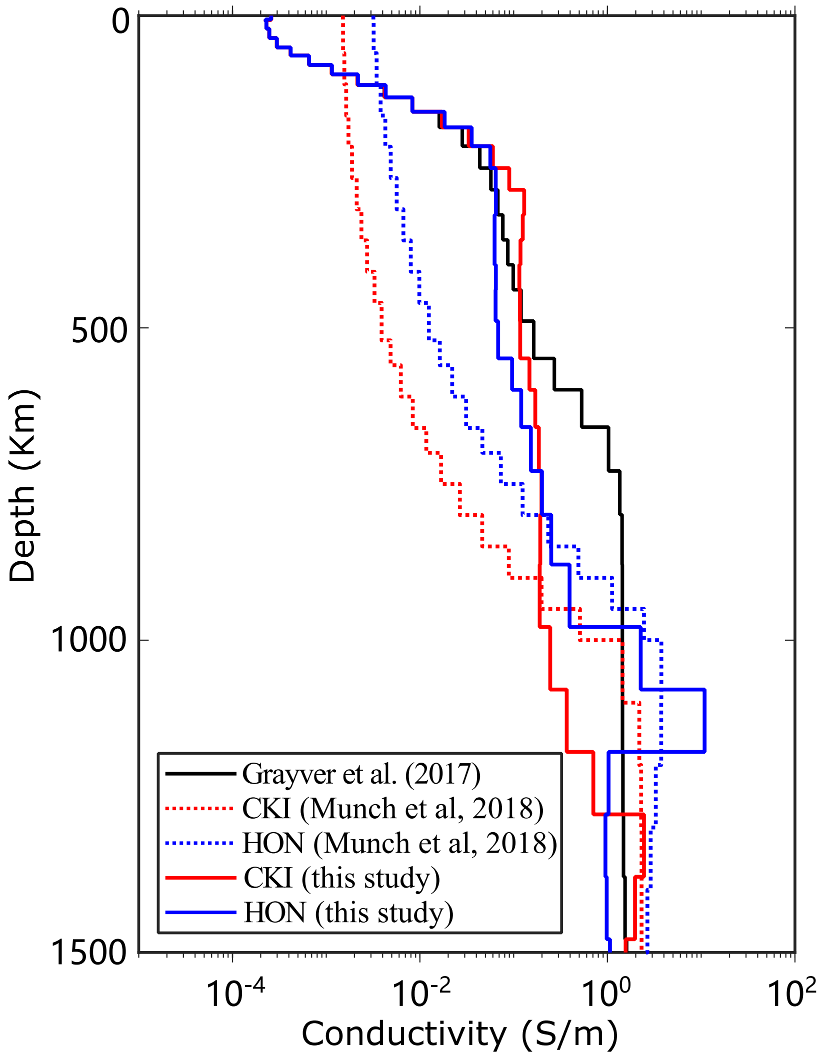

Modeled and observed C-responses at CKI

- C-responses were computed in the model with the 0.01º x 0.01º surface shell and new and old 1-D mantle conductivity profiles underneath CKI.

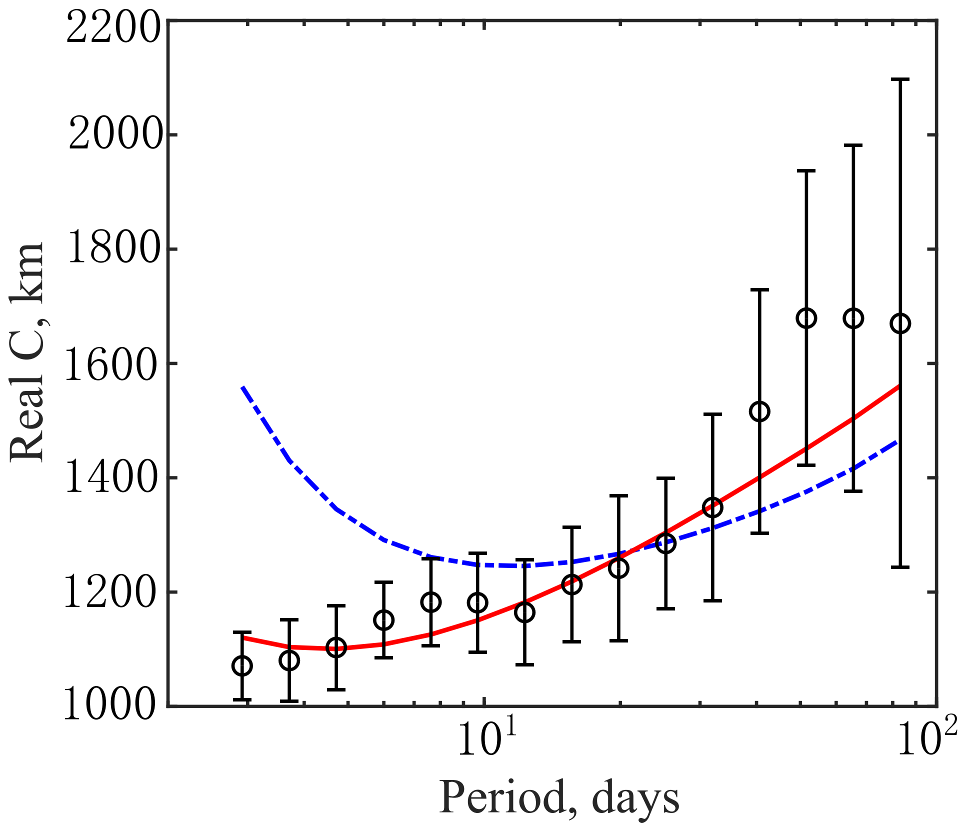

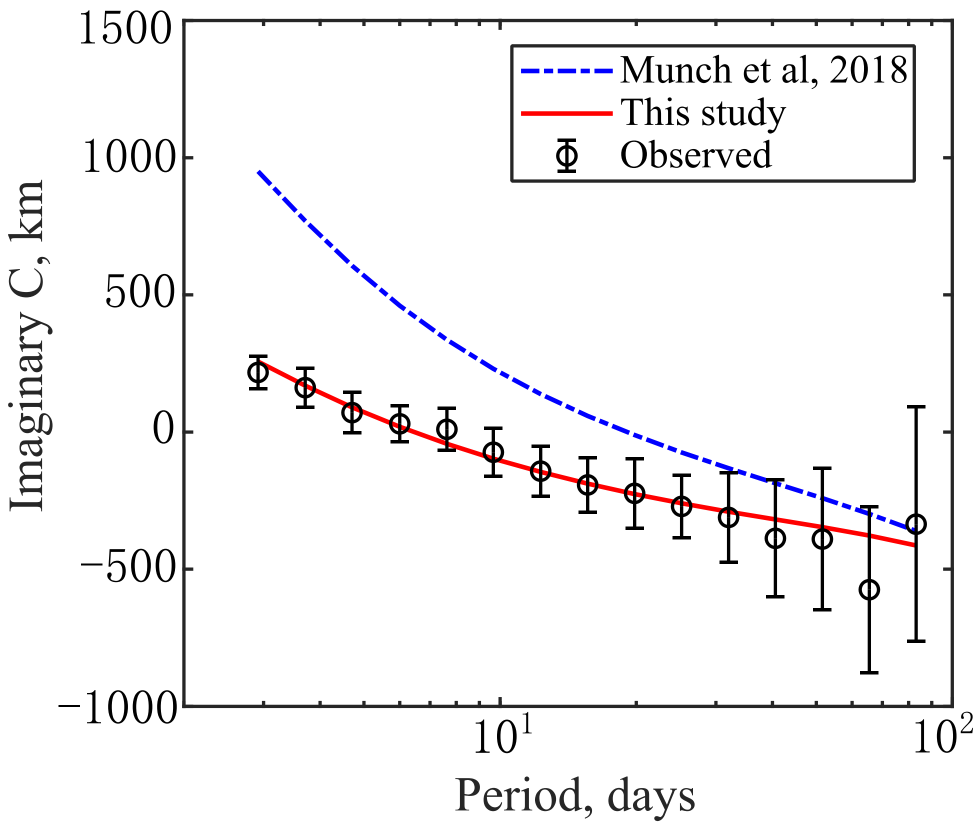

Modeled and observed C-responses at HON

- C-responses were computed in the model with the 0.01º x 0.01º surface shell and new and old 1-D mantle conductivity profiles underneath HON.

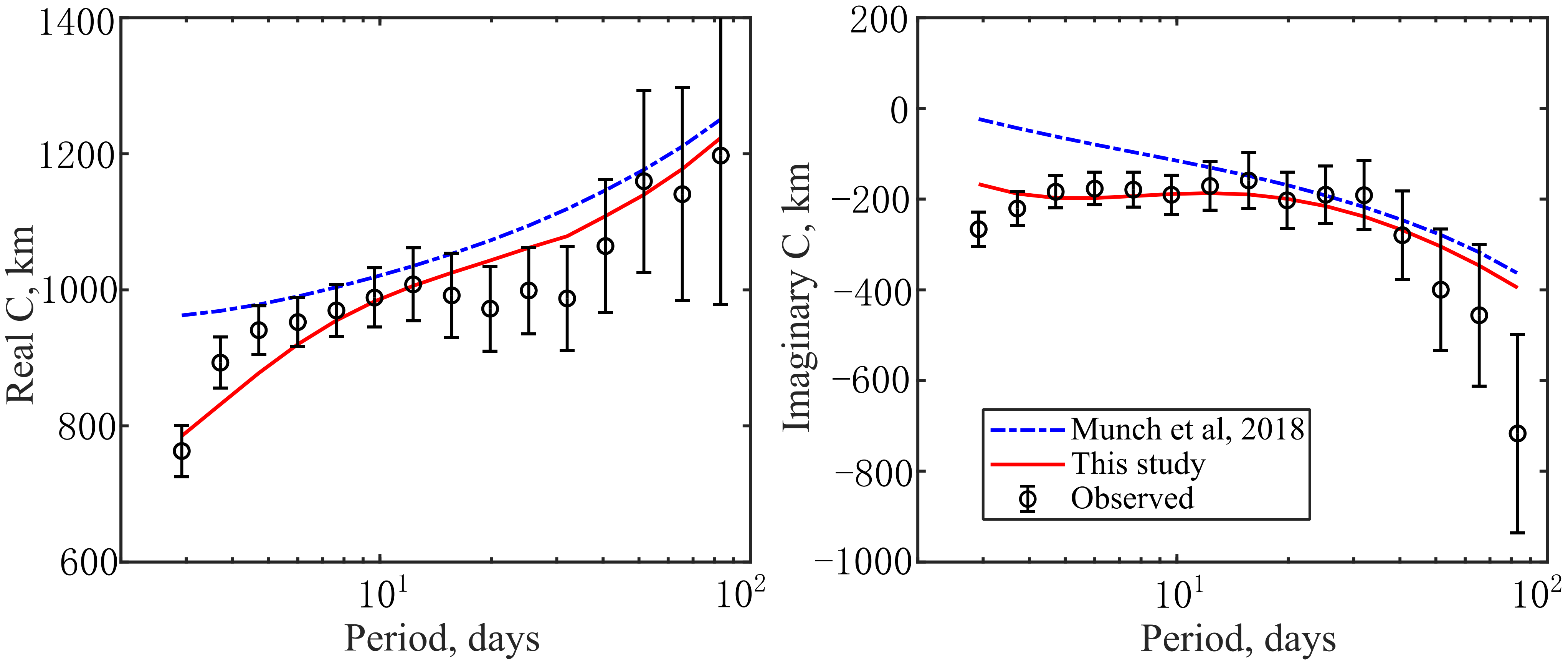

Conclusions

- Global-to-Cartesian 3-D EM modeling method based on a nested IE approach is developed
- Very local bathymetry significantly influences the island C-responses
- We obtain new 1-D conductivity models beneath CKI and HON, and observe impressive agreement between modeled and experimental responses

For more details: Chen, C., Kruglyakov, M., & Kuvshinov, A. (2020). A new method for accurate and efficient modeling of the local ocean induction effects. Application to long-period responses from island geomagnetic observatories. Geophysical Research Letters, 47, doi.org/10.1029.2019GL086351

Outlook

- Joint inversion of MT tippers (Morschhauser et al., 2019), Sq and Dst Global-to-local transfer functions (Püthe et al., 2015; Guzavina et al., 2019) using data from as many island geomagnetic observatories as possible

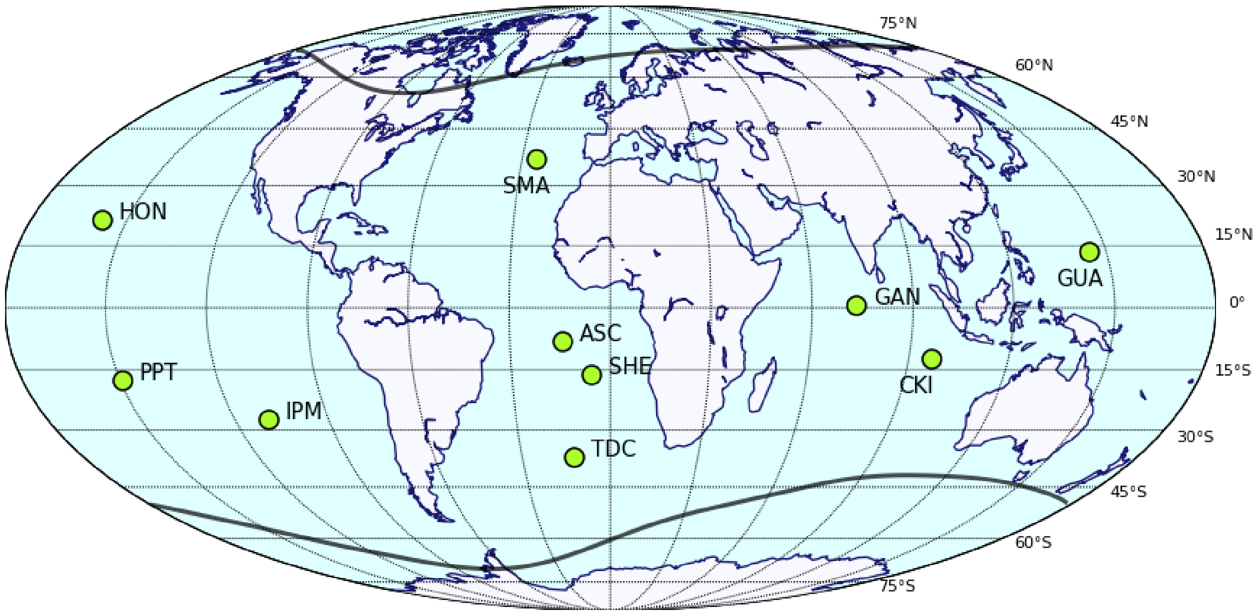

Morschhauser, A., Grayver, A., Kuvshinov, A., Samrock, F., & Matzka, J. Earth, Planets and Space, 2019, 71(1), 17.
Püthe, C., Kuvshinov, A., & Olsen, N. Geophysical Journal International, 2015, 201(1), 318-328.
Guzavina, M., Grayver, A., & Kuvshinov, A. Geophysical Journal International, 2019, 219(3), 2125-2147.